



9th International Conference on Materials Structure and Micromechanics of Fracture

Fracture and Fatigue Behaviour of Implants Made of Ti Alloys

Aleksandar Sedmak^{1*}, Katarina Čolić²

¹*Faculty of Mechanical Engineering, University of Belgrade, Kraljice Marije 16, 11120, Belgrade, Serbia*

²*Innovation Centre of Faculty of Mechanical Engineering, Kraljice Marije 16, 11120, Belgrade, Serbia*

Abstract

This paper presents an analysis of Ti alloys used in biomedical applications, such as artificial joint implants and fixation plates, from a fracture mechanics perspective, including fatigue crack initiation and propagation phenomenon. Toward this end experimental and numerical research of mechanical behaviour of fixation plate and hip replacement implant is presented. Experimental analysis was based on standard methods for testing mechanical properties and application of Digital Image Correlation (DIC) technique, while the Finite Element Method (FEM) was used for numerical simulation. Comparison of results indicated a good agreement of experimental and numerical results and reasonable explanation of fixation plate failure. Experimental and numerical research of cracked hip replacement implant is also presented, including fatigue crack propagation, simulated by the Extended FEM (XFEM) using MORFEO postprocessing of ABAQUS stress-strain results. Based on static analysis and fracture toughness properties, the critical crack length was calculated and then used as the final crack length for fatigue life estimation. Toward this end, the Paris law has been used, with coefficients C and m obtained experimentally on RUMUL testing device. The number of cycles needed for failure which has been obtained was in a reasonable agreement with data from case study analysed.

© 2019 The Authors. Published by Elsevier B.V.

This is an open access article under the CC BY-NC-ND license (<http://creativecommons.org/licenses/by-nc-nd/4.0/>)

Peer-review under responsibility of the scientific committee of the ICMSMF organizers

Keywords: Implants; Ti alloys; Fracture; Fatigue; DIC; FEM; XFEM

1. Introduction

Biomaterials are used for production of medical equipment designed to be implanted into the human body, to replace damaged or diseased body parts. Basically, orthopedic biomaterials should have high levels of yield, tensile and fatigue strength, as well as high corrosion resistance. These characteristics are of great importance in the development of fixating implants which are most often subjected to cyclic loading, Tatic et al (2018), Tatic (2017).

* Corresponding author.

E-mail address: asedmak@mas.bg.ac.rs

Since bones in extremities carry the load, orthopedic plates have to provide support to damaged or broken bones, leading to the natural choice of metallic alloys. Therefore, biomaterial strength and stiffness significantly exceed those of the bones, inevitably leading to so-called shielding effect, Tatic et al (2018), Tatic (2017). Most commonly used metallic biomaterials, Legweel et al (2015), Sedmak et al (2010), for implants are: stainless steels, Co-Cr alloys, and Titanium alloys, the last option being now dominant due to the optimal combination of properties, including the least shielding effect, since it has significantly smaller modulus of elasticity, and the smallest density.

Titanium alloys, Ti-6Al-4V and Ti-6Al-7Nb in particular, represent materials with currently most suitable mechanical properties. Alloy Ti-6Al-4V is made of 90% titanium, 6% aluminium and 4% vanadium, providing high corrosion resistance, high durability, as well as favourable ratio between strength and weight (4.43 g/cm³). Titanium is very resistant to corrosion due to a solid oxide layer (the only stable product of the reaction) which is formed in vivo conditions. Titanium alloys can have different microstructure due to allotropic phases of Ti, closed packed hexagonal (α -Ti), stable up to 882°C, and body centred cubic (β -Ti), stable above it. Monophase alloys have some advantages, but only multiphase alloys can be thermally treated to improve strength.

The main disadvantage of titanium alloys as biomaterials is the fact that they have a high friction coefficient, which can cause particle separation due to wear in the case of direct contact of orthopedic components and tissue. Alloy Ti-6Al-7Nb has a modified chemical composition, containing 7% niobium instead of vanadium, providing even higher corrosion resistance in comparison to Ti-6Al-4V. New type of Ti alloy has more than 10% of Mo to stabilize β phase at room temperature, with basic idea to reduce modulus of elasticity, i.e. the shielding effect. Other attempts to improve Ti-6Al-4V alloy followed the same trace, i.e. Vanadium was replaced with other metals, being less toxic, e.g. Ti-5Al-2.5Fe and Ti-6Al-7Nb, alloys. Several common Ti alloys for biomedical use are presented in Table 1.

Table 1. Standardized Ti alloys

Alloy	Type	UNS number	ASTM standard	ISO standard
Ti-3Al-2.5V	$\alpha + \beta$	R56320	ASTM B 348	
Ti-5Al-2.5Fe	$\alpha + \beta$			ISO 5832-10
Ti-6Al-7Nb	$\alpha + \beta$	R56700	ASTM F 1295	ISO 5832-11
Ti-15Mo	β	R58150	ASTM F 2066	
Ti-13Nb-13Zr	β	R58130	ASTM F 1713	
Ti-12Mo-6Zr-2Fe	β	R58120	ASTM F 1813	

2. Case study – plates for orthopedic fixture

Fracture of orthopedic plates is not so often, but it still happens. The main cause is poor design, i.e. unnecessary high stress concentration in some cases, leading both to static and fatigue failure. Recently, such a case was analysed by Tatic et al (2018), Tatic (2017), even without a crack or crack-like defect. Experimental and numerical evaluation of stress-strain state has been performed by using Digital Image Correlation and Finite Element Method, respectively. In order to eliminate any influence of the small geometrical modifications in the plate design, a new plate was made of a Ti-6Al-4V, with a geometry shown in Figure 1. The plate was cut using the water jet technique to prevent development of potential micro cracks caused by the machining.

Stress-strain field on the surface of the model was measured using digital image correlation-based GOM measuring system, Sedmak et al (2012), Mitrovic et al (2011). The load was gradually increased to a maximum value of 1500 N (corresponding to two times average human weight). Numerical models were created using Abaqus CAE (Dassault Systems, software package). Due to geometrical conditions (double symmetry in geometry and loading conditions), FEM simulation was performed on the quarter of the real model. Models were created as two body models, one representing bone and bolts, the other one the LCP plate, as shown by Tatic et al (2018). Restraints were added on both planes of symmetry (longitudinal and lateral). Loading was positioned in a form of a concentrated force on top and bottom of the connecting pin (purple area), Tatic et al (2018). Compatibility of DIC and FEM models was determined by deformation comparison in the lateral direction between two opposite bolts.

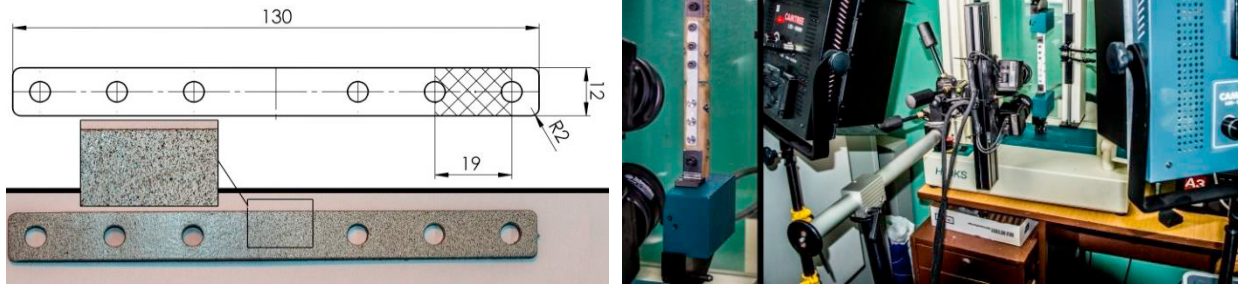


Fig. 1. Scheme of the test plate with enlarged measuring area (left) and experimental set up (right), Tatic et al (2018)

Results for strains, obtained with DIC technology and FEM models, can be seen in Figure 2, indicating good agreement (10% of difference). After the verification of compatibility between FEM and DIC, they were both used to determine Mises stress fields in somewhat different geometry, closer to the real one, Figure 3. The maximum stress in this case is even higher, i.e. 270 MPa, Figure 4. Some differences in distribution of stresses are analysed and explained by Tatic et al (2018).

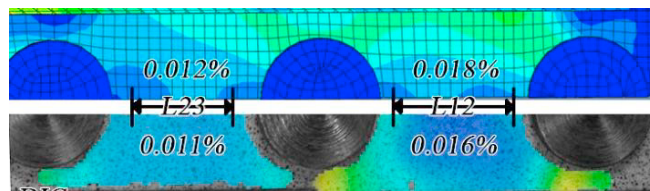


Fig. 2. Deformation field obtained in numerical model (up); results obtained with DIC (bottom), Tatic et al (2018)



Fig. 3. Image of the real plate, broken during patient rehabilitation

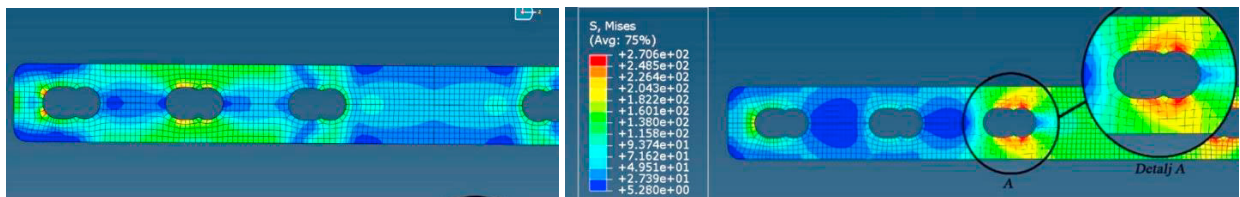


Fig. 4. Stress field obtained in numerical model (left); results obtained with DIC (right)

3. Failure analysis – hip implant

Another typical application of Ti alloys, hip replacement implant, also fails from time to time, either due to static or, more frequently, fatigue loading, Figure 5, as shown by Paliwal (2010) and Chao (2017). Typical static failure is analysed here both experimentally and numerically, following procedure explained by Colic et al (2012), Milovanovic et al (2017), to estimate the stress-strain state, and point out the stress concentration areas. For the experimental part, DIC was used, Mitrovic et al (2011), indicating the most critical areas, Figure 6.



Fig. 5. Typical failures of hip replacement implants

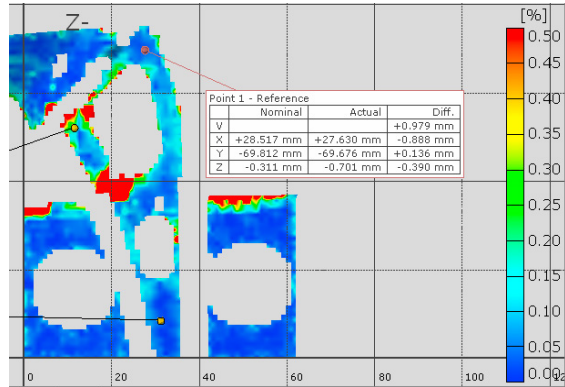


Fig. 6. Experimental setup (left) and results of DIC measurement (right)

The Finite Element Method has been applied to obtain linear elastic stress distribution in hip implant, loaded in the same way as during the experiment, with force of 6 kN, corresponding to stumbling, Colic et al (2017). The mesh is generated so that problem is simulated as realistic as possible. Therefore, the adapter system has been modelled as well, following the solid model. The finite element mesh is shown in Fig. 7, together with stress distribution. The maximum equivalent stress is still in the linear elastic range (698 MPa), enabling simple calculation of the equivalent strain ($698 \text{ MPa} / 120 \text{ GPa} = 0.0058 = 0.58\%$). This is in relatively good agreement with the experimental results, obtained by DIC, shown in Figure 7 (0.5%, indicated by red colour). Also the location of maximum stress/strain is in good agreement (compare Figures 6 and 7b), as well as in good agreement with the typical fracture location, shown in Fig. 5.

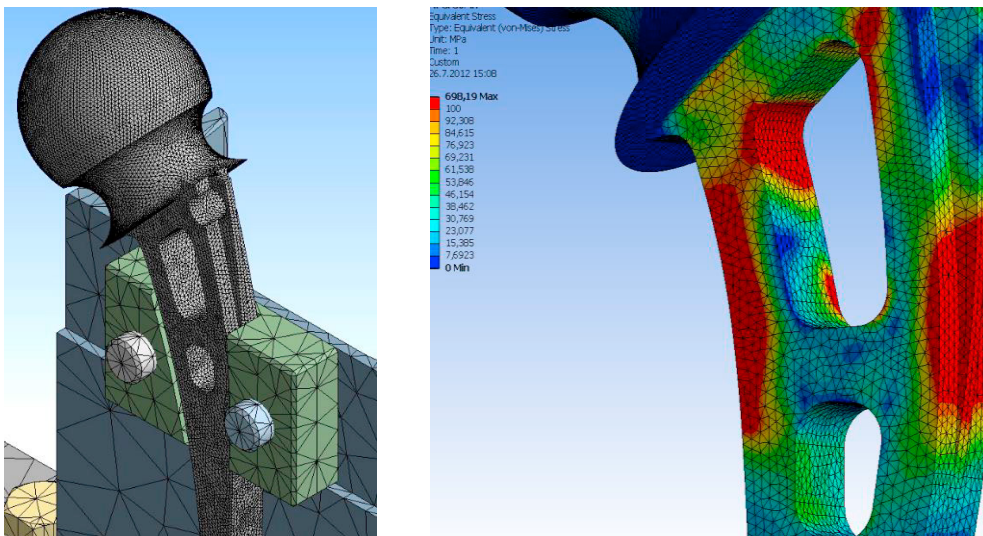


Fig. 7. (a) Finite element mesh, (b) Stress distribution obtained, Colic et all (2017)

4. Fatigue crack propagation

The material fatigue crack growth resistance was determined by applying the ASTM E647 standard procedure [cc] which prescribes measurement of the fatigue crack growth rate da/dN . Experimental testing of Ti-6Al-4V alloy in order to determine the fatigue crack growth rate da/dN and fatigue threshold values ΔK_{th} was performed by using a three point bending specimens on a resonant high frequency RUMUL testing machine. This testing machine achieves variable load torque in the range of -160 to +160 Nm, with a maximum static load of 100 Nm. The test was carried out at the ratio of minimum and maximum load $R = 0.1$. The applied frequency ranged from 215 to 235 Hz. Characteristic diagrams of the fatigue crack growth rate, da/dN , vs. the range of the stress intensity factor, ΔK , for TI-6Al-4V alloy tested at room temperature are shown in Figure 8.

The crack in the numerical model of implant is located at the joint site of the stem with acetabular cup, Figure 9. The behavior of the biomaterial of the artificial hip stem in the presence of a fatigue crack was numerically simulated with an average working force of 2 kN, amplitude stress $2000/176.6 \text{ MPa} = 11.5 \text{ MPa}$.

In the area where crack existence is assumed, a finer mesh is set in relation to the rest of the model, as shown in Figure 10. The initial cracks were placed at the place where fatigue and appearance of microscopic damages are expected to occur, due to the fact that it is a contact surface with other metallic parts of the prosthesis. The numerical calculation was done in the Morfeo/crack for Abaqus software, based on the application of the eXtended Finite Element Method (XFEM), Jovicic et al. Fatigue crack growth was monitored until the failure, as shown in Figure 10 after 10 and 21 steps.

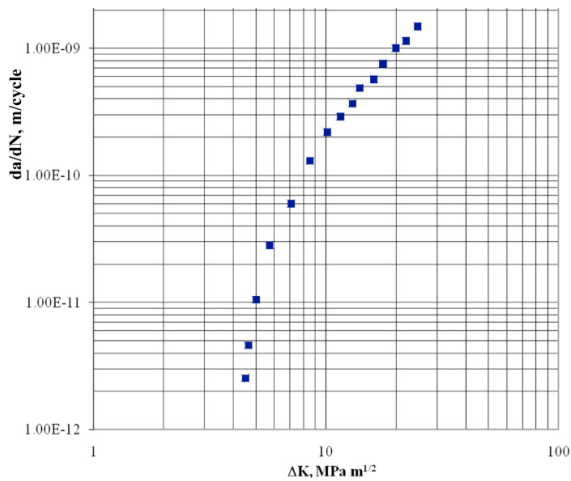


Fig. 8. Diagram for $da/dN - \Delta K$ dependence

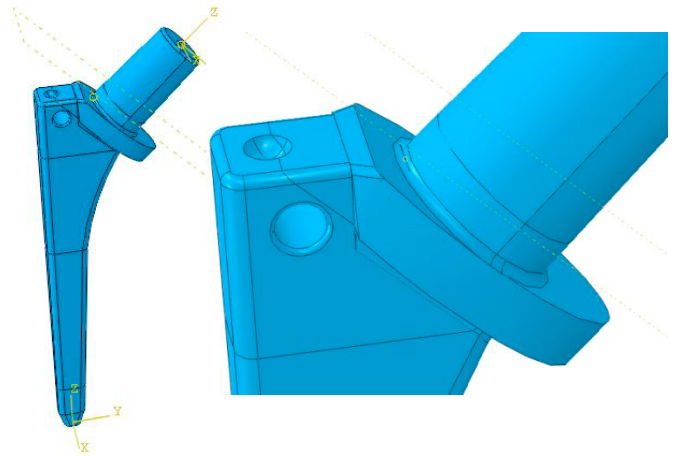


Fig. 9. Representation of the planes of crack positions on the implant

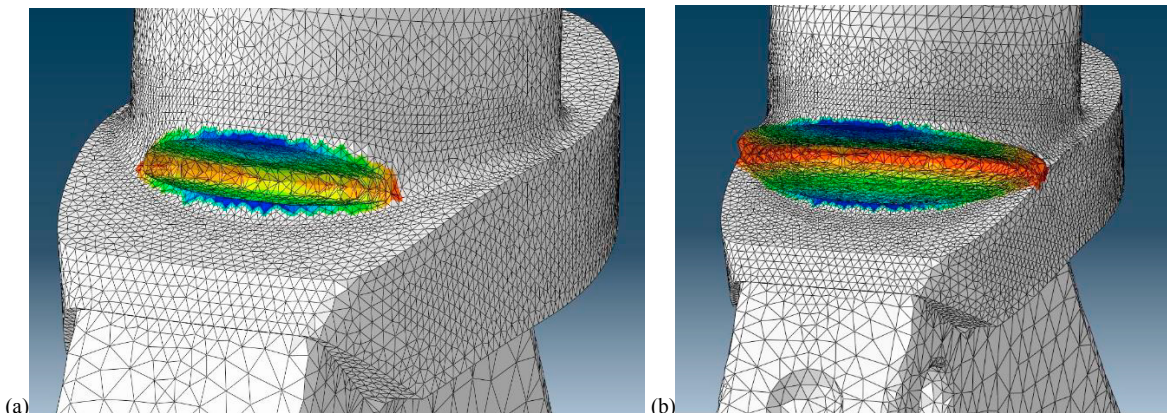


Fig. 10. (a) Maximum value of crack length - step 10, (b) crack growth over the entire length of prosthesis - step 21

The crack length vs. number of cycles, shown in Sedmak et al (2019), indicated that the failure of implant stem will occur after 40 steps of crack growth, since both K_I and crack length start to grow in unstable manner. Corresponding number of cycles is cca 80 Million, which approximates twenty years of active person walking pattern. Experience with hip implant failures indicate that its lifespan is cca 15 years.

For numerical simulation of crack propagation, criterion of linear elastic fracture mechanics were applied, i.e. unstable crack growth is reached in case when K_I reaches K_{Ic} . Applying that, the unstable crack growth will occur after the critical crack length of 18.5 mm, i.e. after 37th step. The critical crack value obtained numerically (18.5 mm) can be well correlated with a_c , determined by simple fracture mechanics analysis, $a_c=16.2$ mm, Sedmak et al (2019).

5. Conclusion

Based on results presented here, one can conclude that fracture and fatigue behavior of implants made of Ti alloys is now well understood and can be analysed successfully with available numerical and experimental methods/tools. More specifically, one can conclude the following:

- In the case of static failure, stress-strain analysis can be used for better design to avoid stress concentration.
- In the case of crack presence, relatively simple fracture and fatigue analysis, based on FEM and XFEM, provides reliable and realistic results.
- In the case of crack propagation under fatigue loading, relatively simple fatigue analysis, based on XFEM, provides also reliable and realistic results.
- More advance methodology should include the spectrum of operating loads that occurs in the real case during the walking cycle and more detailed analysis of the stress intensity factors for the Mode II and III values.

6. Acknowledgment

We acknowledge the support for this investigation by the Ministry for Education, Science and Technological Development, project TR35040 and ON174004. We also thank Prof. Dr. Aleksandar Grbovic who provided insight and expertise that greatly assisted the research.

References

- Tatić, U., Čolić, K., Sedmak, A., Mišković, Z., Petrović, A., 2018. Measuring procedures and evaluation of the stress strain fields on the locking compression plates. *Technical Gazette* 25, 1, 112-117
- Tatić, U., 2017. Analysis of the influence of geometry and biomaterial on orthopedic reconstructive plate integrity and life (in Serbian) doctoral thesis, University of Belgrade
- Legweel K., Sedmak A., Čolić K., Burzić Z., Gubeljak L., 2015. Elastic-Plastic Fracture Behaviour of Multiphase Alloy MP35N. *Structural Integrity and Life*, 15, 163-166.
- Sedmak A., Čolić K., Burzić Z., Tadić S., 2010. Structural Integrity Assessment of Hip Implant Made of Cobalt-Chromium Multiphase Alloy. *Structural Integrity and Life*, 10, 161-164.
- Sedmak A., Milošević M., Mitrović N., Petrović A., Maneski T., 2012. Digital Image Correlation in Experimental Mechanical Analysis. *Structural Integrity and Life*, 12, 39-42
- Paliwal, M., Allan, D.G., Filip, P., 2010. Failure analysis of three uncemented titanium-alloy modular total hip stems. *Engineering Failure Analysis*, 17, 1230–1238.
- Chao J., Lopez V., 2017. Failure analysis of a Ti6Al4V cementless HIP prosthesis. *Engineering Failure Analysis*, 14, 822–830.
- Colic K., Sedmak A., Gubeljak N., Burzic M., Petronic S., 2012. Experimental analysis of fracture behavior of stainless steel used for biomedical applications. *Structural Integrity and Life*, 12, 59-63.
- Milovanović, A., Sedmak, A., Čolić, K., Tatić, U., Đorđević, B., 2017. Numerical analysis of stress distribution in total hip replacement implant, *Structural Integrity and Life*.17, 139–144
- Jovicic, G., Zivkovic, M., Sedmak, A., Jovicic, N., Milovanovic, D., 2010. *Archives of Civil and Mechanical Engineering* 10, 19-35
- Mitrovic, N., Milosevic, M., Sedmak, A., Petrovic, A., Prokic-Cvetkovic, R., 2011. Application and Mode of Operation of Non-Contact Stereometric Measuring System of Biomaterials. *FME Transactions* 39, 55-60
- Čolić, K., Sedmak, A., Legweel, K., Milošević, M., Mitrović, N., Mišković, Z., Hloch, S., 2017. Experimental and Numerical Research of Mechanical Behaviour of Titanium Alloy Hip Implant, *Technical gazette*, Vol. 24, 709-713, June 2017; DOI: 10.17559/TV-20160219132016.
- Sedmak, A., Čolić, A., Grbović, A., Balac, I., Burzić, M., 2019. Numerical Analysis of Fatigue Crack Growth of Hip Implant, *Engineering Fracture Mechanics*, DOI:10.1016/j.engfractmech.2019.10649.